

RESEARCH ARTICLE

An efficient high-power femtosecond laser based on periodic-layered-Kerr media nonlinear compression and a Yb:YAG regenerative amplifier

Jie Guo¹, Zichen Gao^{1,2}, Di Sun^{1,2}, Xiao Du^{1,2}, Yongxi Gao^{1,2}, and Xiaoyan Liang¹

¹State Key Laboratory of High Field Laser Physics, Shanghai Institute of Optics and Fine Mechanics, Chinese Academy of Sciences, Shanghai 201800, China

²Center of Materials Science and Optoelectronics Engineering, University of Chinese Academy of Sciences, Beijing 100049, China

(Received 4 January 2022; revised 28 January 2022; accepted 14 February 2022)

Abstract

We demonstrate an efficient ultrafast source with 195 fs pulse duration, 54 W average power at 200 kHz repetition rate and near diffraction-limited beam quality. The compact setup incorporates a thin-disk Yb:YAG regenerative amplifier (RA) and a subsequent nonlinear pulse compression stage with periodic-layered Kerr media (PLKM), which is one of the multiple-thin-solid-plate schemes based on nonlinear resonator theory. In virtue of the formation of quasi-stationary spatial soliton in PLKM, the near diffraction-limited beam quality of the RA remained almost undisturbed after post-compression. The nonlinear pulse compression module is simple and efficient with a transmission of 96%. To the best of our knowledge, for pulse energy over 200 μJ, this is the highest output power reported for the multiple-thin-solid-plate scheme. This source manifests an economical combination to mitigate the bandwidth limitations of Yb-based high-power chirped pulse amplifiers.

Keywords: high-power ultrafast source; post-compression; self-phase modulation

1. Introduction

The combination of high quantum and Stokes efficiency of Yb-based lasers with state-of-the-art fiber, Innoslab and thin-disk architectures facilitates efficient and power scalable femtosecond lasers^[1–5]. However, the Yb-doped gain matrices do not exhibit sufficiently large gain bandwidth to provide high gain for pulses shorter than 300 fs. Due to gain narrowing, workhorse Yb-doped crystals, such as Yb:YAG and Yb:tungstate, typically generate pulses in the range from 400 fs to 1 ps pulse duration after chirped pulse amplification. To generate even shorter pulses, other strategies have proved viable, such as the adoption of broader gain bandwidth disordered media^[6,7], a combination of gain media with a slightly shifted gain spectrum^[8–10] or spectral coherent synthesis^[11,12]. Nonetheless, the disordered media display poor thermal conductivity while the other two

schemes suffer from complexity. Nonlinear spectral broadening by self-phase modulation (SPM) during propagations in regenerative and multi-pass amplifiers is an impressive alternative, which, however, demands elaborated control^[13–16].

In addition to the above techniques implemented during the construction of ultrafast lasers, another route to achieve shorter pulse durations is through the well-known temporal compression after compressor approach (CafCA) or post-compression technique^[17–19]. The basic process incorporates nonlinear spectral broadening and chirp removal with dispersive elements. No laser system alteration is needed and a high efficiency can be guaranteed if implemented properly. Among the various techniques based on the optical Kerr effect or photoionization for spectral broadening, the gas-filled multi-pass cell spectral broadening (MPCSB) and the multiple-thin-solid-plate (MTSP) schemes now are widely adopted and have achieved impressive results^[20–23]. The MPCSB method is characterized with almost unperturbed beam quality and spectral homogeneity across the beam profile, but suffers from pointing fluctuations and delay^[24]. The MTSP technique avoids the catastrophic collapse

Correspondence to: X. Liang, State Key Laboratory of High Field Laser Physics, Shanghai Institute of Optics and Fine Mechanics, Chinese Academy of Sciences, Shanghai 201800, China. Email: liangxy@siom.ac.cn

caused by the self-focusing effect in a bulk medium with strategically arranged thin plates. It is more compact, flexible and economical, applicable for peak power far beyond the medium's self-focusing critical power and for pulse energies up to the millijoule level with robustness and reproducible performance^[25]. Early MTSP configurations were usually organized empirically, in which considerable losses caused by conical emission usually arose^[26]. The conical emission also results in temporal or spatial (or even both) quality degradation. In some cases requirements for specially designed chirped mirrors or pulse shapers were indispensable^[20,26]. As a relatively systematical study, the concept of quasi-stationary spatial solitons generation in periodic-layered Kerr media (PLKM) stands out as a practical strategy^[27,28]. As the term periodic indicates, the distance between neighboring plates is the same in this configuration. Specifically, a layer of solid thin plate with thickness of l and a layer of free space with a length of L were taken as a period. The repetitive propagation of an intense beam in PLKM was regarded as a resonator with intensity-dependent non-spherical mirrors. Thus, the Fresnel–Kirchhoff diffraction (FKD) integral was introduced in this theory to identify the self-consistent stationary modes. The PLKM arrangements improved the spatial quality and supported nonlinear light–matter interaction during a rather long distance even under tight focusing conditions^[28]. The integration of a PLKM device and Yb-based high-power chirped pulse amplifiers (CPAs) will favor an ultrafast source with high efficiency and great beam quality.

In this contribution, we present a compact and efficient ultrashort laser source, which comprised a Yb:YAG regenerative amplifier (RA) and a subsequent close-to-lossless PLKM-based nonlinear pulse compression stage. The nonlinear pulse compression stage featured a transmission of 96%, excellent beam quality and spectral homogeneity across the beam profile. Compared with the setup described in Ref. [26], there is no need to filter out the conical emission or apply custom-tailored chirped mirrors in our work. The absence of conical emission intrinsically ensured the high efficiency and excellent beam quality simultaneously. To the best of our knowledge, for pulse energy over 200 μJ , this is the highest output power reported for the MTSP scheme. This configuration successfully compensated for the gain bandwidth limitation of Yb:YAG RA. The final output pulse duration was 195 fs with average power of 54 W at a 200 kHz repetition rate, while the pulse duration directly from the grating-based compressor of the CPA system was 534 fs. These results underline the benefits of this combination. The demonstrated source is promising for further power scaling and compression to sub-50 fs to drive high-field physical processes and bright secondary radiation at high average power.

2. Experimental setup

A schematic of the experimental setup is illustrated in Figure 1. The Yb:YAG thin-disk RA was similar to that in our previous work^[29]. Different from the system in Ref. [29], the Pockels cell was a double-BBO (beta-barium borate) type with a total length of 40 mm and a clear aperture of 3.6 mm \times 3.6 mm (4 mm \times 4 mm total area), and the pump spot size on the disk was 3 mm. Limited by the high-voltage pulse width of the Pockels cell, the roundtrip number of the RA was set as 15. Besides, the grating compressor is based on a single transmission grating and some folding mirrors. When seeded with 100 μJ pulse energy, an output energy of 330 μJ at 200 kHz was generated at the pump power of 150 W. The compressed pulse energy was then reduced to 280 μJ and the beam quality factor was characterized as $M^2 = 1.19 \times 1.24$ (Ophir BeamSquared), as shown in Figure 2. The output spectrum bandwidth was about 3.6 nm (full width at half maximum, FWHM), revealing a strong gain-narrowing phenomenon. The pulse duration was measured to be 534 fs with pedestals assuming a Lorentz pulse shape (shown in Figure 4(b) of the following section), larger than the bandwidth-limited one (factor ~ 1.2). This is attributed to the nonlinear effects of the front end, which is also not bandwidth-limited with 325 fs pulse duration at 8 nm bandwidth. In contrast, the nonlinearity accumulated in the RA is negligible (about 0.11 rad).

The PLKM setup for nonlinear spectral broadening consisted of six periods. Each period includes a layer of sapphire with a fixed nominal thickness of 1 mm and a subsequent layer of free space with a length of 40.8 mm. The PLKM device was designed as follows. Firstly, the nonlinear phase on each solid thin plate was set as 1 rad and the effective beam radius on each plate was decided. The value was chosen to limit the nonlinear phase per plate and fully exploit the plates (six pieces) available in the experiment. Then, the FKD integral, including the nonlinear phase induced by SPM, was numerically solved by means of Fox–Li iteration, resulting in the determination of stationary modes^[28,30]. When the normalized amplitude of the incident optical field is assumed as U_1 , the amplitude after propagating through a unit of the nonlinear resonator and right before the next period can be calculated according to Ref. [28]:

$$U_2(\rho) = -2\pi j e^{j\pi\rho^2} \int_0^\infty U_1(\rho') e^{jb|U_1(\rho')|^2} \cdot e^{j\pi\rho'^2} \cdot J_0(2\pi\rho'\rho) \rho' d\rho,$$

where ρ and ρ' are the radial coordinates rescaled by $\sqrt{\lambda L}$ and J_0 is the zeroth-order Bessel function. In this equation, b is the nonlinear phase given by $b = \frac{2\pi}{\lambda} n_2 I_0$, in which n_2 is the nonlinear refractive index and I_0 is the field intensity. After convergence, the Fresnel-number-like radius squared

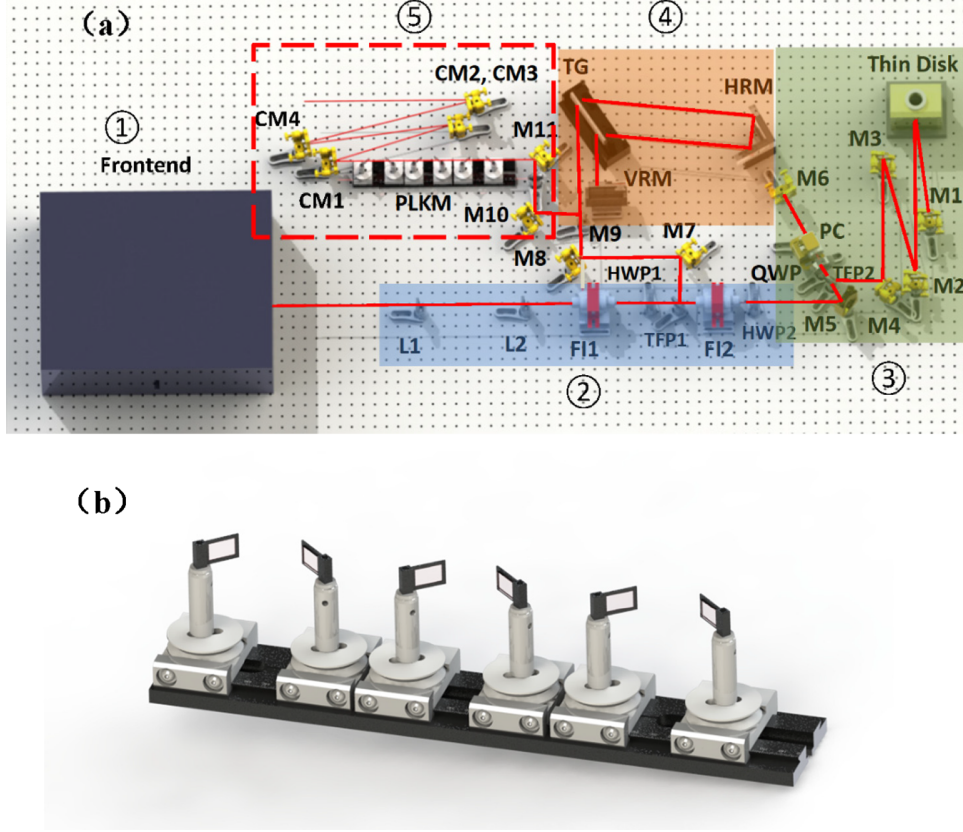


Figure 1. (a) Schematic of the ultrafast source: ① frontend; ② mode matching optics and isolators; ③ regenerative amplifier; ④ grating compressor; ⑤ PLKM nonlinear compression stage. L1, L2, lenses of the telescope for mode matching; FI, Faraday isolator; TFP, thin-film polarizer; M1–M11, highly reflective mirrors; HWP, half-wave plate; QWP, quarter-wave plate; PC, Pockels cell; HRM, horizontal roof mirror; VRM, vertical roof mirror; TG, transmission grating; CM1–CM4, chirped mirrors. (b) Detailed PLKM configuration.

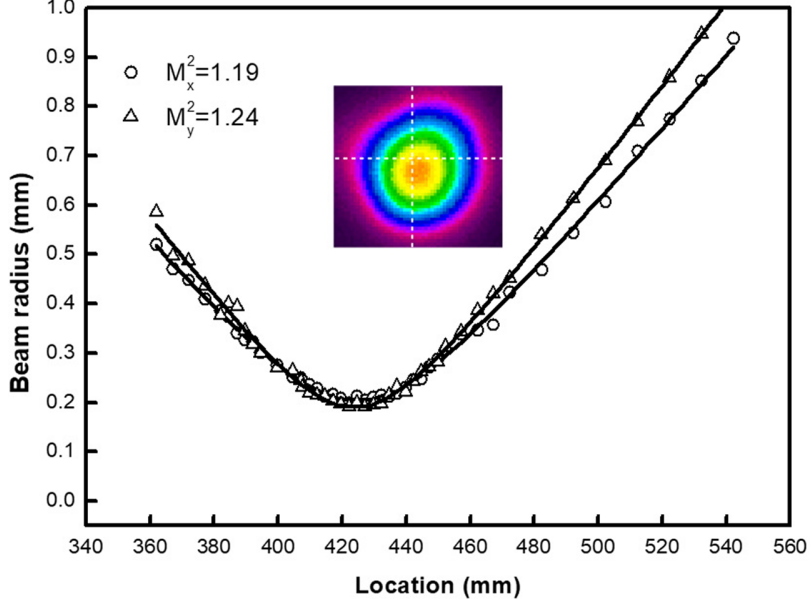


Figure 2. Output beam quality and far-field beam profile after the grating compressor.

parameter $\omega^2/\lambda L$ was found to be 0.78 when 86.5% energy was contained, in which ω is the beam radius and λ is the central wavelength of 1030 nm.

The sapphire plates were placed at the Brewster angle to suppress the reflection loss to less than 0.5%. The first sapphire plate was placed at the beam focus and the peak

intensity on the surface of the first plate was 0.84 TW/cm^2 . A set of dispersive mirrors (supporting a bandwidth of 40 nm) with a total group delay dispersion (GDD) of $-15,370 \text{ fs}^2$ compensated for the residual spectral phase.

3. Nonlinear compression results and discussion

The transmitted average power behind the nonlinear compression stage was 54 W, corresponding to an efficiency of 96%. This high efficiency is attributed to the lossless nature of PLKM and the dispersive mirror compressor. Figure 3(a) shows the power spectra measured with an integrating sphere and a multimode fiber at the output of the RA and after the PLKM stage, respectively. Spectra measured after different numbers of sapphire thin plates are illustrated in Figure 3(b). The broadening to the input spectrum is slightly asymmetrical. In addition, the amplitude of spectral broadening at the short-wavelength part is a little larger than the long-wavelength part, indicating the emergence of a weak self-steepening effect. The oscillations with large amplitude near the center wavelength were caused by the temporal pedestals of the input pulse^[17], which stems from the nonlinear effects

of the front end and, in addition, the spectra after the plates were modulated. Its influence upon the pulse stability was also confirmed. The fluctuation of pulse energy was 1% root mean square (RMS) and the variation of pulse duration was within 5%. This spectral modulation will be improved with an optimized front end in the near future.

The broadened spectrum with six plates spans from 1020 to 1040 nm (-20 dB), supporting a 140 fs transform limited pulse. The autocorrelation trace characterized at the final output is shown in Figure 4(a), indicating a pulse duration of 195 fs assuming a Gaussian pulse shape, which is, however, quite clean without pedestals, unlike the input pulse (Figure 4(b)). It is presumed that the SPM of the input nonlinearly chirped pulse produced a third order dispersion (TOD) with the opposite sign to the initial TOD^[31]. These results verified that the nonlinear compression stage realized contrast improvement and spectral broadening simultaneously. The transform-limited pulse duration was not achieved, presumably due to the residual high-order spectral dispersion, which remained uncompensated with the dispersive mirrors. The residual high-order spectral dispersion originated from both the front end and the self-steepening effect of the nonlinear compression stage^[31,32].

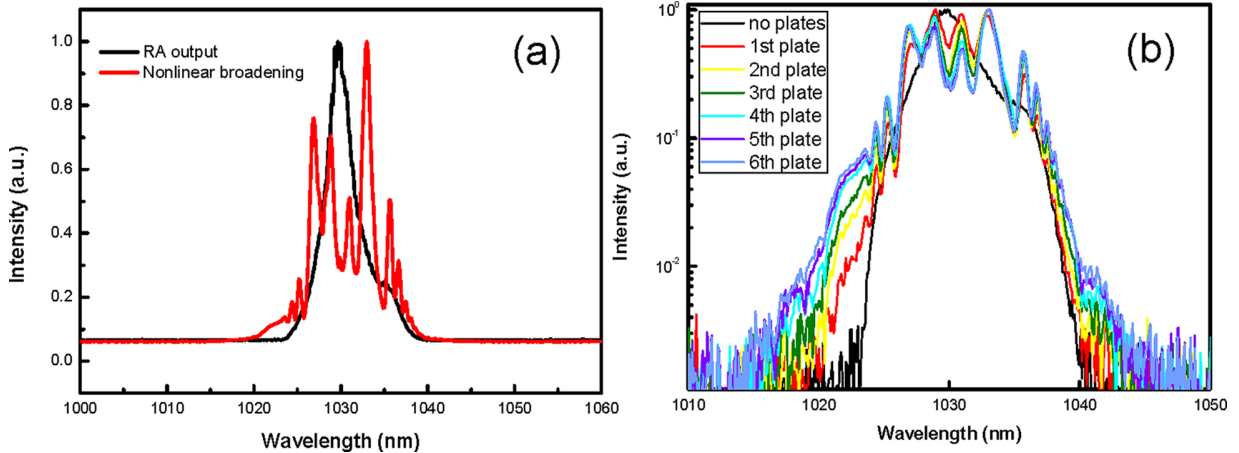


Figure 3. (a) Spectra measured at the output of the RA and after the PLKM. (b) Spectra measured after different numbers of sapphire thin plates.

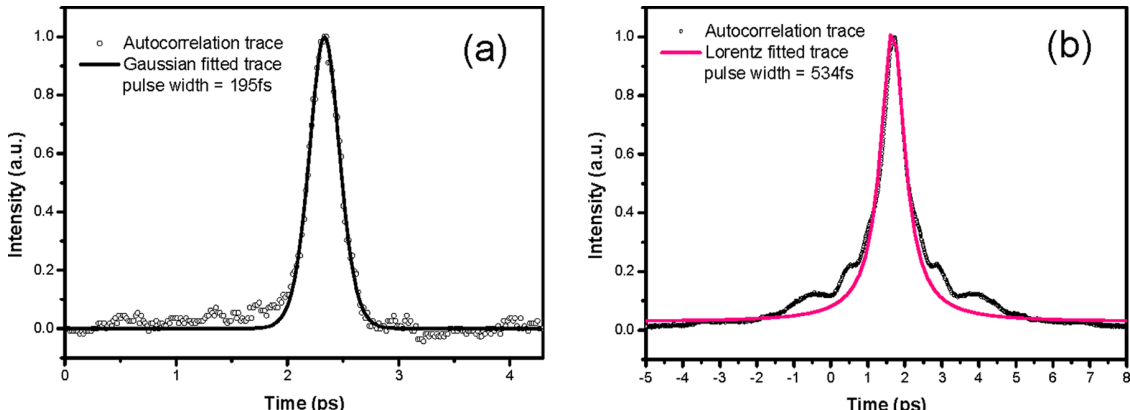


Figure 4. Measured and fitted intensity autocorrelation traces of (a) the final output pulse and (b) the output of the grating compressor.

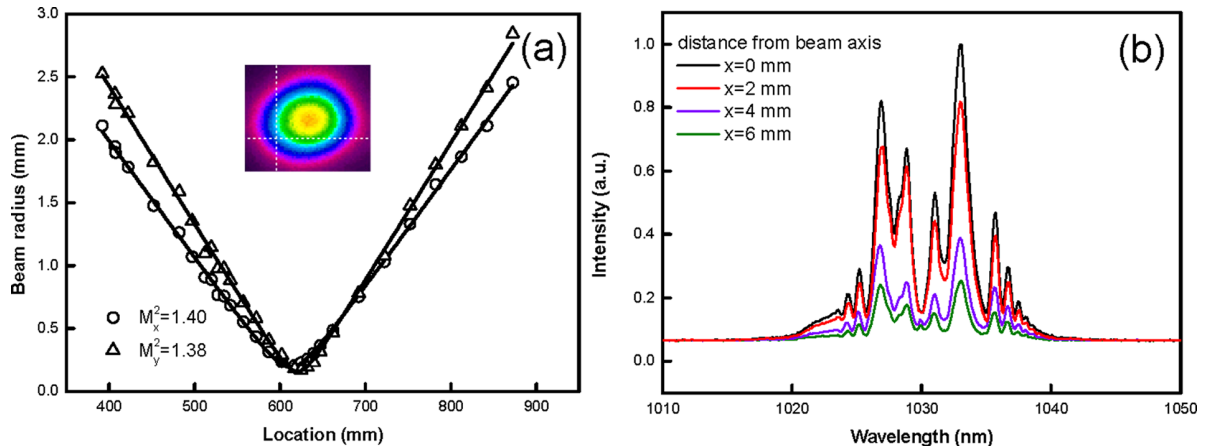


Figure 5. (a) The final output beam quality and far-field beam profile. (b) Spectra across the beam profile.

The spatial quality of the nonlinear compression stage was also examined. The beam quality factor was measured to be $M^2 = 1.40 \times 1.38$, which is shown in Figure 5(a). In addition, the homogeneity of spectral broadening was also characterized by measuring the spectra across the transverse beam profile of the final compressed beam, at the location with a beam diameter of about 12 mm. A multimode fiber was used to scan across the profile and spectra were recorded with an optical spectrum analyzer (Figure 5(b)). It is generally expected that nonlinear spectral broadening by free-space propagation through a nonlinear medium will be inhomogeneous across the beam profile. The output beam quality and spectral homogeneity confirmed the validity of the basic scheme based on PLKM theory, that is, by restricting the nonlinear phase accumulation of each plate and regarding propagation through each period as roundtrips in a nonlinear resonator. The operation parameters are fundamentally determined beforehand, making it easy to implement in practice. In our experiment, only slight adjustment of distances between plates was needed. No conical emission was observed during the experiment; thus, great beam quality and high transmission efficiency were guaranteed. A small amount of remaining spatial chirp and uncompensated high-order dispersion were also shown in our results, which will be further optimized by an improved setup with modified front end and thinner plates in the nonlinear compression stage.

4. Summary

In summary, we have demonstrated a laser system delivering an average power of 54 W and pulses with 195 fs duration at a repetition rate of 200 kHz. The nonlinear compression stage helped to achieve a pulse duration well below the conventional bandwidth-limited value, enhancing the peak power of the Yb:YAG high-power CPA system by 2.6 times, with great beam quality and spectral homogeneity across

the beam profile. These results confirmed the potential of the PLKM-based technique for the efficient and economical compression of high average power laser amplifiers at high repetition rates. Such source presents a favorable and robust tool for novel manufacturing mechanisms and time-resolved spectroscopy experiments^[33–36].

Acknowledgments

This work was supported by the National Key Research and Development Program of China (2017YFB0405202), the National Natural Science Foundation of China (NSFC) (62005298) and the Program of Shanghai Academic/Technology Research Leader (20SR014501).

References

1. H. Stark, J. Buldt, M. Mueller, A. Klenke, and J. Limpert, Opt. Lett. **46**, 969 (2021).
2. C. Roecker, A. Loescher, F. Bienert, P. Villevall, D. Lupinski, D. Bauer, A. Killi, T. Graf, and M. A. Ahmed, Opt. Lett. **45**, 5522 (2020).
3. T. Nubbemeyer, M. Kaumanns, M. Ueffing, M. Gorjan, A. Alismail, H. Fattahi, J. Brons, O. Pronin, H. G. Barros, Z. Major, T. Metzger, D. Sutter, and F. Krausz, Opt. Lett. **42**, 1381 (2017).
4. P. Russbeldt, D. Hoffmann, M. Hofer, J. Lohring, J. Luttmann, A. Meissner, J. Weitenberg, M. Traub, T. Sartorius, D. Esser, R. Wester, P. Loosen, and R. Poprawe, IEEE J. Sel. Top. Quantum Electron. **21**, 3100117 (2015).
5. P. Russbeldt, T. Mans, J. Weitenberg, H. D. Hoffmann, and R. Poprawe, Opt. Lett. **35**, 4169 (2010).
6. E. Caracciolo, A. Guandalini, F. Pirzio, M. Kemnitzer, F. Kienle, A. Agnesi, and J. A. der Au, Proc. SPIE **10082**, 100821F (2017).
7. E. Kaksis, G. Almasi, J. A. Fulop, A. Pugzlys, A. Baltuska, and G. Andriukaitis, Opt. Express **24**, 28916 (2016).
8. U. Buenting, H. Sayinc, D. Wandt, U. Morgner, and D. Kracht, Opt. Express **17**, 8046 (2009).
9. G. H. Kim, J. H. Yang, D. S. Lee, A. V. Kulik, E. G. Sall, S. A. Chizhov, U. Kang, and V. E. Yashin, J. Opt. Technol. **80**, 142 (2013).

10. A. Buettner, U. Buenting, D. Wandt, J. Neumann, and D. Kracht, Opt. Express **18**, 21973 (2010).
11. N. B. Chichkov, U. Buenting, D. Wandt, U. Morgner, J. Neumann, and D. Kracht, Opt. Express **17**, 24075 (2009).
12. F. Guichard, M. Hanna, L. Lombard, Y. Zaouter, C. Honninger, F. Morin, F. Druon, E. Mottay, and P. Georges, Opt. Lett. **38**, 5430 (2013).
13. M. Ueffing, R. Lange, T. Pleyer, V. Pervak, T. Metzger, D. Sutter, Z. Major, T. Nubbemeyer, and F. Krausz, Opt. Lett. **41**, 3840 (2016).
14. B. Dannecker, J.-P. Negel, A. Loescher, P. Oldorf, S. Reichel, R. Peters, T. Graf, and M. A. Ahmed, Opt. Commun. **429**, 180 (2018).
15. J. Pouysegur, M. Delaigue, C. Honninger, P. Georges, F. Druon, and E. Mottay, Opt. Express **22**, 9414 (2014).
16. J. Pouysegur, M. Delaigue, Y. Zaouter, C. Honninger, E. Mottay, A. Jaffres, P. Loiseau, B. Viana, P. Georges, and F. Druon, Opt. Lett. **38**, 5180 (2013).
17. T. Nagy, P. Simon, and L. Veisz, Adv. Phys. X **6**, 1845795 (2021).
18. P. Balla, A. B. Wahid, I. Sytcevich, C. Guo, A.-L. Viotti, L. Silletti, A. Cartella, S. Alisauskas, H. Tavakol, U. Grosse-Wortmann, A. Schoenberg, M. Seidel, A. Trabattoni, B. Manschewitz, T. Lang, F. Calegari, A. Couairon, A. L'Huillier, C. L. Arnold, I. Hartl, and C. M. Heyl, Opt. Lett. **45**, 2572 (2020).
19. E. A. Khazanov, S. Y. Mironov, and G. Mourou, Phys. Uspekhi **62**, 1096 (2019).
20. C. H. Lu, Y. J. Tsou, H. Y. Chen, B. H. Chen, Y. C. Cheng, S. D. Yang, M. C. Chen, C. C. Hsu, and A. H. Kung, Optica **1**, 400 (2014).
21. P. Russbueldt, J. Weitenberg, J. Schulte, R. Meyer, C. Meinhardt, H. D. Hoffmann, and R. Poprawe, Opt. Lett. **44**, 5222 (2019).
22. J. Schulte, T. Sartorius, J. Weitenberg, A. Vernaleken, and P. Russbueldt, Opt. Lett. **41**, 4511 (2016).
23. C. L. Tsai, F. Meyer, A. Omar, Y. Wang, A. Y. Liang, C. H. Lu, M. Hoffmann, S. D. Yang, and C. J. Saraceno, Opt. Lett. **44**, 4115 (2019).
24. J. Weitenberg, A. Vernaleken, J. Schulte, A. Ozawa, T. Sartorius, V. Pervak, H.-D. Hoffmann, T. Udem, P. Russbueldt, and T. W. Haensch, Opt. Express **25**, 20502 (2017).
25. P. He, Y. Liu, K. Zhao, H. Teng, X. He, P. Huang, H. Huang, S. Zhong, Y. Jiang, S. Fang, X. Hou, and Z. Wei, Opt. Lett. **42**, 474 (2017).
26. C. H. Lu, W. H. Wu, S. H. Kuo, J. Y. Guo, M. C. Chen, S. D. Yang, and A. H. Kung, Opt. Express **27**, 15638 (2019).
27. S. N. Vlasov, V. A. Petrishchev, and V. I. Talanov, Appl. Opt. **9**, 1486 (1970).
28. S. Zhang, Z. Fu, B. Zhu, G. Fan, Y. Chen, S. Wang, Y. Liu, A. Baltuska, C. Jin, C. Tian, and Z. Tao, Light Sci. Appl. **10**, 53 (2021).
29. D. Sun, J. Guo, W. Wang, X. Du, Y. Gao, Z. Gao, and X. Liang, IEEE Photonics J. **13**, 3900110 (2021).
30. A. G. Fox and T. Li, IEEE J. Quantum Electron. **2**, 774 (1966).
31. A. Suda and T. Takeda, Appl. Sci. Basel **2**, 549 (2012).
32. M. Trippenbach and Y. B. Band, Phys. Rev. A **57**, 4791 (1998).
33. R. R. Gattass and E. Mazur, Nat. Photonics **2**, 219 (2008).
34. D. Kiselev, L. Woeste, and J. P. Wolf, Appl. Phys. B **100**, 515 (2010).
35. R.-T. Liu, X.-P. Zhai, Z.-Y. Zhu, B. Sun, D.-W. Liu, B. Ma, Z.-Q. Zhang, C.-L. Sun, B.-L. Zhu, X.-D. Zhang, Q. Wang, and H.-L. Zhang, J. Phys. Chem. Lett. **10**, 6572 (2019).
36. K. E. Knowles, M. D. Koch, and J. L. Shelton, J. Mater. Chem. C **6**, 11853 (2018).